

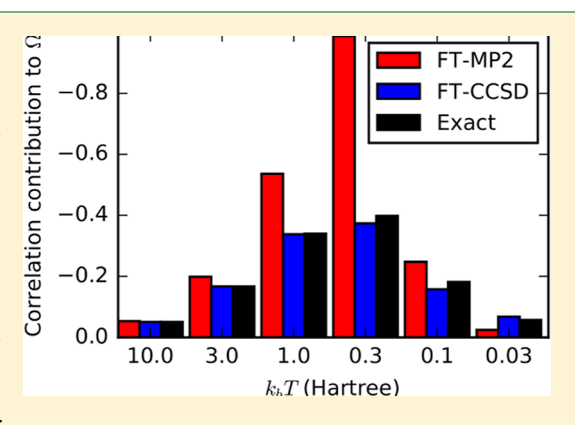
A Time-Dependent Formulation of Coupled-Cluster Theory for Many-Fermion Systems at Finite Temperature

Alec F. White* and Garnet Kin-Lic Chan*

Division of Chemistry and Chemical Engineering, California Institute of Technology, Pasadena, California 91125, United States

Supporting Information

ABSTRACT: We present a time-dependent formulation of coupled cluster theory. This theory allows for direct computation of the free energy of quantum systems at finite temperature by imaginary time integration and is closely related to the thermal cluster cumulant theory of Mukherjee and co-workers [Chem. Phys. Lett. 1992, 192, 55–61; Phys. Rev. E 1993, 48, 3373–3389; Chem. Phys. Lett. 2001, 335, 281–288; Chem. Phys. Lett. 2002, 352, 63–69; Int. J. Mod. Phys. B 2003, 17, 5367–5377]. Our derivation of the finite-temperature theory highlights connections to perturbation theory and to zero-temperature coupled cluster theory. We show explicitly how the finite-temperature coupled cluster singles and doubles amplitude equations can be derived in analogy with the zero-temperature theory and how response properties can be efficiently computed using a variational Lagrangian. We discuss the implementation for realistic systems and showcase the potential utility of



the method with calculations of the exchange correlation energy of the uniform electron gas under warm dense matter conditions.

1. INTRODUCTION

In calculations of the electronic structure of molecules and materials, the effects of a finite electronic temperature are usually not considered. This is sufficient for nearly all molecular systems and for many systems in the condensed phase, because only a small number of electronic states are thermally populated at typical temperatures. However, there are cases where the electronic temperature plays a crucial role. In correlated electron materials, interactions lead to low-energy electronic excitations and electronic phase transitions. 1-5 Differences in the electronic free energy can also drive structural transitions, both in molecules, such as in spin crossover complexes, and in crystals. Hot electrons can be used to drive new types of reactions, as seen in hot electron-driven chemistry on plasmonic nanoparticles.8 And finally, the properties of materials under extreme conditions,9 including at high electronic temperatures, 10 is also of interest for a variety of applications. For all these problems, a quantum many-body theory at finite temperature is required, and this has led to renewed interest in computational approaches.

The simplest treatment of many-body systems is mean field theory, and mean field theory at finite temperature, in the form of Hartree–Fock¹¹ or density functional theory (DFT), ^{12,13} is routinely used. In recent years, experimental interest in matter at high temperatures has spurred much activity in finite-temperature DFT. ^{14–17} However, a description of electron correlations beyond the mean-field/DFT level is often required for accurate computation of chemical and material properties. Methods for the approximate treatment of correlations based

on finite-temperature perturbation theory and finite-temperature (Matsubara) Green's functions have been known for many years, 18-20 and there has been some recent interest in applying these techniques in an ab initio context.^{21,22} They are commonly used as impurity solvers within dynamical mean field theory (DMFT)^{5,23,24} and the related dynamical cluster approximation (DCA). 1-4,25 Finite-temperature quantum Monte Carlo (QMC) methods such as determinantal QMC and path integral Monte Carlo (PIMC) have also been studied for many years. 26-30 However, for Fermionic systems, QMC methods display a sign problem, limiting simulations to high temperatures, or requiring the introduction of additional constraints, such as the fixed node approximation in PIMC (called restricted PIMC (RPIMC)). 31,32 There has been recent work to explore formulations of QMC where the sign problem is less severe under the conditions of interest, including the configuration path integral Monte Carlo (CPIMC)³³ and density matrix quantum Monte Carlo (DQMC).34,35 Much of this research has been motivated by calculations on the uniform electron gas for the benchmarking and/or parametrization of finite temperature density functionals. 17,36,37 We will return to this topic in Section 4.2.

The coupled cluster method, which is widely used for its accuracy at zero temperature, ^{38–42} has not seen widespread application at finite temperatures. Kaulfuss and Altenbokem were the first to try to extend coupled cluster theory to finite

Received: July 26, 2018 Published: September 27, 2018

5690

temperatures by means of an exponential ansatz for the density matrix.⁴³ However, their formalism requires knowledge of the spectrum of the interacting Hamiltonian and is therefore illsuited to computations on realistic systems. Mukherjee and coworkers have developed a more practical method, which they have termed the thermal cluster cumulant (TCC) method. 44-48 This method is based on a thermally normal ordered exponential ansatz for the interaction picture imaginary-time propagator. The TCC method has a formal similarity to single reference and multireference coupled cluster theories, but the applications have been limited to very small systems and semianalytical problems. Hermes and Hirata have recently presented a finite-temperature coupled cluster doubles (CCD) method⁴⁹ based on "renormalized" finite-temperature perturbation theory.⁵⁰ Hummel has independently developed a timedependent coupled cluster theory,⁵¹ which is closely related to Hirata's renormalized perturbation theory. We will discuss some aspects of these methods in Section 2.2.

In this paper, we present an explicitly time-dependent formulation of coupled cluster theory applicable to calculations at zero or finite temperature. Imaginary time integration generates a coupled cluster approximation to the thermodynamic potential in the Grand Canonical ensemble. This theory, which we will call finite-temperature coupled cluster (FT-CC), represents the finite temperature analogue of traditional coupled cluster, in that it has the same diagrammatic content. We highlight this fact by showing how the theory may be derived directly from many-body perturbation theory. This theory is also equivalent to a particular realization of the TCC method. In addition to the theory, we discuss the implementation including analytic derivatives for response properties. Some benchmark calculations are presented as a means of validating the implementation and evaluating the accuracy of the method. Finally, we present calculations of the exchange-correlation energy of the uniform electron gas (UEG) under conditions in the warm dense matter regime.

2. THEORY

2.1. Finite-Temperature Coupled-Cluster Equations.

Before discussing the details of the derivation of the FT-CC equations, it is instructive to state the result and discuss the analogy with the zero-temperature theory. Conventional, zerotemperature, coupled-cluster theory has been described in detail in a variety of reviews and monographs. 39,41,52,53 We will review the basic aspects of the theory in order to facilitate comparison with the finite-temperature theory developed in this paper. Recall that the coupled-cluster method can be derived from an exponential wave function ansatz:

$$|\Psi_{\rm CC}\rangle = e^T |\Phi_0\rangle \tag{1}$$

where $|\Phi_0\rangle$ is a single determinant reference. The *T*-operator is defined in some space of configurations, $\{\Phi_u\}$, such that

$$T = \sum_{\mu} t_{\mu} a_{\mu} \tag{2}$$

where t_u is an amplitude and a_u is an excitation operator, such

$$a_{\mu}|\Phi_{0}\rangle = |\Phi_{\mu}\rangle \tag{3}$$

Generally, the T-operator is truncated at some finite excitation level. For example, letting $T = T_1 + T_2$ yields the coupled-cluster singles and doubles (CCSD) approximation. The coupled-cluster energy and amplitudes are then determined from a projected Schrodinger equation:

$$\langle \Phi_0 | e^{-T} H e^T | \Phi_0 \rangle = E_{HF} + E_{CC} \tag{4}$$

$$\langle \Phi_{\mu} | e^{-T} H e^{T} | \Phi_{0} \rangle = 0 \tag{5}$$

These equations can be written explicitly in terms of the Tamplitude and molecular integral tensors using diagrammatic methods^{38,53} or computer algebra. The correlation contribution to the energy has a particularly simple form, in terms of the T_1 and T_2 amplitudes:

$$E_{\text{CC}} = \sum_{ia} t_i^a f_{ia} + \frac{1}{4} \sum_{ijab} \langle ij || ab \rangle (t_{ij}^{ab} + 2t_i^a t_j^b)$$
 (6)

Although this wave-function-based derivation is usually favored, the resulting energy has a well-understood connection to perturbation theory (see, for example, Chapters 9.4 and 10.4 of ref 53).

In finite-temperature coupled-cluster theory, we use an explicitly time-dependent formulation. The time-dependent analogues of the T-amplitudes are functions of an imaginary time τ , and will be denoted by $s_u(\tau)$. At finite temperature and chemical potential, we denote the coupled-cluster contribution to the grand potential as $\Omega_{\rm CC}$, such that, given a particular reference,

$$\Omega = \Omega^{(0)} + \Omega^{(1)} + \Omega_{CC} \tag{7}$$

The coupled-cluster contribution is given by

$$\Omega_{\text{CC}} = \frac{1}{4\beta} \sum_{ijab} \langle ij||ab \rangle \int_0^\beta d\tau \left[s_{ij}^{ab}(\tau) + 2s_i^a(\tau) s_j^b(\tau) \right]
+ \frac{1}{\beta} \sum_{ia} f_{ia} \int_0^\beta d\tau s_i^a(\tau) + \frac{1}{\beta} \sum_{ia} f_{ia} \int_0^\beta d\tau s_i^a(\tau)$$
(8)

where β is the inverse temperature. In the limit $\beta \to \infty$, eq 8 reduces to

$$\lim_{\beta \to \infty} \Omega_{\text{CC}} = \frac{1}{4} \sum_{ijab} \langle ij||ab \rangle \lim_{\tau \to \infty} [s_{ij}^{ab}(\tau) + 2s_i^a(\tau)s_j^b(\tau)] + \sum_{ia} f_{ia} \lim_{\tau \to \infty} s_i^a(\tau)$$
(9)

In this limit, $\Omega \to E - \mu N$. For an insulator, the correlation contribution to N will vanish at zero temperature, assuming that μ can be chosen such that the noninteracting and correlated systems have the same number of particles. This requires the noninteracting and correlated energy gaps to have nonvanishing overlap, which is typically the case, from which it follows that

$$\lim_{\beta \to \infty} \Omega_{\rm CC} = E_{\rm CC} \tag{10}$$

Comparing eq 9 with eq 6, it is clear that

$$\lim_{\tau \to \infty} s_i^a(\tau) = t_i^a \quad \lim_{\tau \to \infty} s_{ij}^{ab}(\tau) = t_{ij}^{ab} \tag{11}$$

This is true as long as both amplitudes correspond to the same solution of the nonlinear amplitude equations. This correspondence also implies that the $\beta \to \infty$ limit of these timedependent amplitudes is related to the imaginary-time version of the amplitudes that appear in time-dependent, wave function-based coupled-cluster formulations.⁵⁶

The FT-CC amplitude equations closely resemble the amplitude equations of zero-temperature coupled cluster, and they are diagrammatically identical, as we will discuss in Section 2.3. This allows the equations to be written in precise analogy with the zero-temperature amplitude equations:

- replace t_{μ} with $s_{\mu}(\tau')$
- for each contraction, sum over all orbitals instead of just occupied or virtual orbitals
- include an occupation number from the Fermi–Dirac distribution $(n_i \text{ or } 1 n_a)$ with each index not associated with an amplitude
- multiply each term by -1
- for each term contributing to $s_{\mu}(\tau)$, multiply by an exponential factor $\exp[\Delta_{\mu}(\tau'-\tau)]$ and integrate τ' from 0 to τ

As an example, we compare the zero-temperature and finite-temperature versions of a term linear in T_1 (or $S_1(\tau')$ at finite temperature), which contributes to T_2 (or $S_2(\tau)$ at finite temperature):

$$t_{ij}^{ab} \leftarrow \frac{1}{\Delta_{ij}^{ab}} P(ij) \sum_{c} \langle ab || cj \rangle t_{i}^{c}$$
(12)

$$s_{ij}^{ab}(\tau) \leftarrow -P(ij) \sum_{c} (1 - n_a)(1 - n_b) n_j \langle ab | lcj \rangle$$

$$\times \int_0^{\tau} d\tau' e^{(\epsilon_a + \epsilon_b - \epsilon_i - \epsilon_j)(\tau' - \tau)} s_i^c(\tau')$$
(13)

The full FT-CCSD amplitude equations are given in Appendix A. We discuss the origin of these specific rules in Sections 2.3 and 2.4.

2.2. Perturbation Theory at Zero and Finite Temperature. Perturbation theory for the many-body problem has a long history in chemistry and physics. Time-independent Rayleigh—Schrodinger perturbation theory, time-dependent (or frequency-dependent) many-body perturbation theory at zero temperature, and imaginary time-dependent (or imaginary frequency-dependent) many-body perturbation theory at finite temperature have been discussed in a variety of monographs. ^{18–20,53,61,62} For completeness, in Appendix B, we give explicit rules for the diagrammatic derivation of time-domain expressions for the shift in the grand potential in the form most relevant to coupled-cluster theory. As an example, applying these rules at second order yields

$$\Omega^{(2)} = \frac{1}{4\beta} \sum_{ijab} |\langle ij||ab\rangle|^2 n_i n_j (1 - n_a) (1 - n_b)$$

$$\times \left[\frac{\beta}{\varepsilon_i + \varepsilon_j - \varepsilon_a - \varepsilon_b} + \frac{1 - e^{\beta(\varepsilon_i + \varepsilon_j - \varepsilon_a - \varepsilon_b)}}{(\varepsilon_i + \varepsilon_j - \varepsilon_a - \varepsilon_b)^2} \right]$$

$$+ \frac{1}{\beta} \sum_{ia} |f_{ai}|^2 n_i (1 - n_a) \left[\frac{\beta}{\varepsilon_i - \varepsilon_a} + \frac{1 - e^{\beta(\varepsilon_i - \varepsilon_a)}}{(\varepsilon_i - \varepsilon_a)^2} \right]$$
(14)

In this expression, all sums run over all orbital indices. We use f_{pq} and $\langle pq||rs\rangle$ to indicate the one-particle and antisymmetrized, two-particle elements of the interaction. We have analytically performed the time integrals to obtain the final, time-independent expressions.

The terms containing exponential factors vanish when summed. However, one must be careful when evaluating the terms where the energy denominators appear to vanish. Such cases were called "anomalous" by Kohn and Luttinger, ⁶³ and they require special consideration to obtain the proper finite result. Since each term is an integral of a nonsingular function over a finite interval, each term in the sum should be individually finite. We explicitly include the exponential factors in this discussion, so that eq 14 is finite term-by-term for finite β . The second-order correction can diverge as $\beta \to \infty$, but such divergences are well-known in systems that are metallic at zeroth order. In such cases, finite-temperature perturbation theory will not reduce to perturbation theory at zero temperature, as first observed by Kohn and Luttinger. ⁶³ This is hardly surprising, since the two perturbation theories compute different quantities. This is particularly clear if we express the second-order energy corrections in terms of derivatives of the exact energy E, with respect to a coupling constant λ :

$$E_{\text{MP2}} = \frac{\partial^2 E}{\partial \lambda^2} \bigg|_{\lambda = 0, N} \qquad E_{\text{FT-MP2}} = \frac{\partial^2 E}{\partial \lambda^2} \bigg|_{\lambda = 0, \mu} . \tag{15}$$

For a metallic system, the derivative at fixed μ will differ from the derivative at fixed N, even as $T \to 0$, simply because the chemical potentials of the Hartree–Fock reference system and the interacting system are different. Santra and Schirmer published a pedagogical discussion that elaborates on this particular aspect of finite-temperature perturbation theory. ⁶⁴

In light of this discussion, it is clear that the distinction between the two quantities in eq 15, termed the Kohn–Luttinger conundrum by Hirata and He, 50 does *not* imply any particular problem with FT-MBPT; it simply reflects the different conditions under which the partial derivative is taken, from the different ensembles in the zero- and finite-temperature theories. For this reason, we do not discuss the "renormalized" finite-temperature MBPT of Hirata and He 50 and the related coupled-cluster doubles method, 49 which incorrectly modify finite-temperature perturbation theory to force these two derivatives to be the same in the limit of zero temperature.

2.3. Time-Dependent Coupled Cluster from Perturbation Theory. The interpretation of coupled-cluster theory in the context of many-body perturbation theory can be used to directly define FT-CC theory. The essential point is to require that the energy and amplitude equations reproduce exactly the diagrammatic content of the zero-temperature theory. However, the time-dependent perturbation theory generally will necessitate the consideration of different time orderings. Consider the open diagrams shown in Figure 1 as an example.

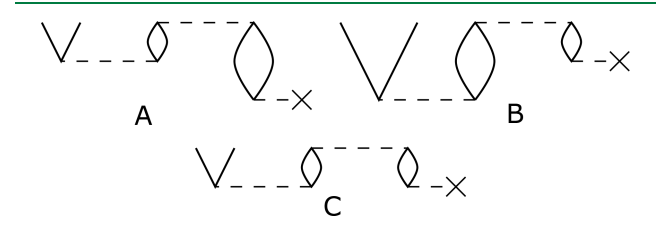


Figure 1. Different time orderings of a term relevant to CCSD.

We must consider both diagrams A and B, and each corresponds to nested integrals of the form

$$A \approx v_{bc}^{jk}(\tau) \int_0^\tau \mathrm{d}\tau' f_j^b(\tau') \int_0^{\tau'} \mathrm{d}\tau'' v_{ki}^{ca}(\tau'') \tag{16} \label{eq:16}$$

$$B \approx \nu_{bc}^{jk}(\tau) \int_0^{\tau} d\tau' \nu_{ki}^{ca}(\tau') \int_0^{\tau'} d\tau'' f_j^b(\tau'')$$
(17)

where we have omitted the summation and the factors of occupation numbers, which will be common in both terms. We have used $v_{rs}^{pq}(\tau)$ and $f_{vq}(\tau)$ to represent the one and twoelectron matrix elements in the interaction picture:

$$\nu_{rs}^{pq}(\tau) \equiv \langle pq | lrs \rangle e^{(\varepsilon_p + \varepsilon_q - \varepsilon_r - \varepsilon_s)\tau}
f_{pq}(\tau) \equiv f_{pq} e^{(\varepsilon_p - \varepsilon_q)\tau}$$
(18)

These nested integrals can be simplified in a manner analogous to the factorization of perturbation theory denominators in coupled cluster at zero temperature. (See Chapters 5-6 in ref 53.) By defining

$$V_{rs}^{pq}(\tau) \equiv \int_0^{\tau} d\tau' v_{rs}^{pq}(\tau') \qquad F_{pq}(\tau) \equiv \int_0^{\tau} d\tau' f_{pq}(\tau')$$
(19)

such that

$$f_{pq}(\tau) = \frac{\mathrm{d}}{\mathrm{d}\tau} F_{pq}(\tau) \qquad v_{rs}^{pq}(\tau) = \frac{\mathrm{d}}{\mathrm{d}\tau} V_{rs}^{pq}(\tau)$$
 (20)

The reverse of the product rule can be applied to the sum of the two time orderings to yield an expression where all quantities are evaluated at a single time:

$$A + B \propto \nu_{bc}^{jk}(\tau) F_j^b(\tau) V_{ki}^{ca}(\tau)$$
(21)

which we represent as diagram C of Figure 1. This is the timedomain equivalent of the denominator factorization that allows zero-temperature coupled-cluster diagrams to be written without regard to the ordering of the different factors of T. Given this factorization, we may define S-amplitudes at first order, such that

$$s_i^a(\tau)_{\rm I}^{[1]} \equiv -n_i(1-n_a)F_{ai}(\tau)$$
 (22)

$$s_{ij}^{ab}(\tau)_{I}^{[1]} \equiv -n_{i}n_{j}(1-n_{a})(1-n_{b})V_{ij}^{ab}(\tau)$$
(23)

where we use the subscript "I" to emphasize that we are using the interaction picture. The superscript indicates that they are first order in the interaction. The finite-temperature coupledcluster equations at some truncated order (usually singles and doubles) then follow directly from their diagrammatic representation. This guarantees by construction that the FT-CC amplitude equations reproduce the diagrammatic content of the corresponding zero temperature theory exactly.

For the purposes of this derivation, we have used the interaction picture. However, there is a numerical difficulty associated with the time-dependent exponential factors which, at long times, will be become exponentially large or small. This leads to problems of overflow or underflow when storing the amplitudes as floating point numbers. This difficulty can be largely overcome by moving to the Schrodinger picture:

$$s_{\mu}(\tau) \equiv s_{\mu}(\tau)_{\rm I} e^{-\Delta_{\mu} \tau} \tag{24}$$

At first order, the Schrodinger-picture singles and doubles amplitudes are proportional to the Schrodinger-picture matrix elements, which are time-independent in the usual case. Furthermore, these amplitudes are well-behaved in the limit as $\tau \to \infty$, in that they reduce to the zero-temperature coupledcluster amplitudes. The FT-CCSD amplitude equations for the Schrodinger-picture amplitudes are given in Appendix A.

2.4. Relationship to Thermal Cluster Cumulant **Theory.** The finite-temperature coupled-cluster method that we have presented here can also be viewed as a particular realization of the thermal cluster cumulant (TCC) theory developed by Mukherjee and others. 44-48 If we denote the thermal normal ordering of a string of operators by $N[\cdots]_0$, then the TCC method uses a normal-ordered ansatz for the

imaginary-time propagator:

$$U_{\rm I}(\tau) = N[e^{S(\tau) + X(\tau)}]_0$$
 (25)

Here, $S(\tau)$ is an operator and $X(\tau)$ is a number. The imaginary time propagator obeys a Bloch equation,

$$-\frac{\partial U_{\rm I}}{\partial \tau} = V_{\rm I}(\tau)U_{\rm I}(\tau) \tag{26}$$

from which differential equations for $S(\tau)$ and $X(\tau)$ may be determined. The expression for the thermodynamic potential follows directly from the ansatz of eq 25:

$$\Omega = \Omega^{(0)} - \left(\frac{1}{\beta}\right) X(\beta) \tag{27}$$

As shown in ref 45, eq 26 implies coupled differential equations for S and X. Solving these equations by integration yields the FT-CC equations

$$X(\tau) = -\tau \Omega^{(1)} - \int_0^{\tau} d\tau' [V_I^N(\tau)N[e^{S(\tau)}]_0]_{\text{fully contracted}}$$
(28)

$$S(\tau) = -\int_0^{\tau} d\tau' [V_I^N N[e^{S(\tau)}]_0]_C$$
 (29)

 $V_{\rm I}^{\rm N}(\tau)$ is the thermally normal-ordered component of the interaction, and the first-order contribution to the free energy, $\Omega^{(1)}$, is the number component of *V*. The subscript "C" in eq 29 indicates that we only consider terms in which V is connected to all the amplitudes by at least one contraction. Inserting eq 28 into eq 27 yields the first-order contribution to the grand potential plus the interaction picture version of the FT-CC contribution to the grand potential (eq 8). A minor difference is that, in our formulation, we have absorbed the occupation numbers into the definition of the S-amplitudes, whereas in the TCC method, the occupation numbers arise as a result of thermal contractions involving the S operators. The connected cluster form of eq 29 leads to the same set of diagrams obtained in coupled cluster. When properly interpreted, these diagrams reproduce the FT-CC amplitude equations in the interaction picture. Using the relation

$$S(\tau) = S_1(\tau) + S_2(\tau) \tag{30}$$

leads to the FT-CCSD method that we have described.

2.5. Response Properties. The primary utility of the thermodynamic potential is that differentiation will generate ensemble averages. In practice, we most often require the average energy, entropy, and number of particles:

$$\langle E \rangle = \Omega + T \langle S \rangle + \mu \langle N \rangle$$
 (31)

$$\langle S \rangle = -\frac{\partial \Omega}{\partial T} \qquad \langle N \rangle = -\frac{\partial \Omega}{\partial \mu}$$
 (32)

The partial derivatives in eq 32 are partial thermodynamic derivatives but still require the inclusion of the response of any parameters that determine the form of Ω . Generally, an

observable corresponding to an operator O can be computed by defining a new Hamiltonian,

$$H[\alpha] \equiv H + \alpha O \tag{33}$$

and taking the derivative of the thermodynamic potential

$$\langle O \rangle = \frac{\mathrm{d}\Omega[\alpha]}{\mathrm{d}\alpha} \bigg|_{\alpha=0} \tag{34}$$

Just like the coupled-cluster energy at zero temperature, $\Omega_{\rm CC}$ is not a variational function of the amplitudes. This complicates the implementation of analytic derivatives, but this difficulty can be largely mitigated by using a variational Lagrangian, as in the zero-temperature theory. ^{52,53,65} The finite-temperature free-energy and amplitude equations have the form

$$s_{\mu}(\tau) + \int_{0}^{\tau} d\tau' e^{\Delta_{\mu}(\tau' - \tau)} S_{\mu}(\tau') = 0$$
 (35)

$$\frac{1}{\beta} \int_0^\beta E(\tau) = \Omega_{\rm CC} \tag{36}$$

The precise forms of E and S are given in Appendix A. The computation of properties can be simplified by defining a Lagrangian, \mathcal{L} , with Lagrange multipliers $\lambda^{\mu}(\tau)$,

$$\mathcal{L} \equiv \frac{1}{\beta} \int_0^\beta E(\tau) - \frac{1}{\beta} \int_0^\beta d\tau \, \lambda^{\mu}(\tau) \left[s_{\mu}(\tau) + \int_0^\tau d\tau' \, e^{\Delta_{\mu}(\tau - \tau)} S_{\mu}(\tau') \right]$$
(37)

such that variational optimization of \mathcal{L} , with respect to the λ -amplitudes, yields the FT-CC amplitude equations. Variational optimization, with respect to the S-amplitudes, yields equations for λ^{μ} . The solution of the FT-CC λ -equations is discussed in Appendix C.

Once the λ -amplitudes have been determined, any first-order property may be computed from the partial derivative of the Lagrangian. In practice, the specifics of the numerical evaluation of the time integrals must be considered. Some details of the implementation of analytic derivatives are discussed in Appendix C.

3. IMPLEMENTATION

We have developed a simple pilot implementation of FT-CCSD interfaced to the PySCF electronic structure package. In our implementation, the numerical integration is performed on a uniform grid using Simpson's rule for the quadrature weights (see Appendix D for details). Although effective at high temperatures, this integration scheme is far from optimal at low temperatures and can be improved considerably by taking into account the structure of the S amplitudes at low temperature. For example, we know that

$$\lim_{\tau \to 0} s_{\mu}(\tau) = 0 \tag{38}$$

$$\lim_{\tau \to \infty} s_{\mu}(\tau) = [\text{constant}] \tag{39}$$

and this information can be used to develop much more efficient quadrature schemes at low temperatures. However, we have not pursued this in this work.

In our implementation, the integrals are contracted with the occupation numbers once before the start of the iterations. A guess for the S amplitudes is obtained from the MP2 amplitudes or from a previous calculation. Using the modified integrals and the guess, the coupled cluster iterations proceed in two steps. First, $S1_i^a(\tau')$ and $S2_{ii}^{ab}(\tau')$ of eqs A-5 and A-6 are evaluated at

each time point. Second, these quantities are integrated as described in Appendix D to obtain new amplitudes. In our implementation, we compute the amplitudes for all times at each iteration. It is possible to invert this algorithm so that the amplitudes are converged in a point-by-point manner, starting with $\tau=0$. The number of iterations needed to achieve convergence is strongly temperature-dependent: more iterations are generally required at lower temperatures. In practice, it is also sometimes necessary to damp the iterations to achieve convergence at lower temperatures. Direct inversion of the iterative subspace (DIIS) convergence acceleration 67–69 could potentially be used to accelerate convergence at the cost of additional storage.

We used the formulation of Stanton and Gauss⁷⁰ to implement the amplitude equations efficiently. Similar intermediates are used in the solution of the λ -equations. At low temperatures, the FT-CCSD equations can be somewhat simplified in that summations over all orbitals can be restricted to those terms, where the products of occupation numbers are non-negligible. In other words, if $1-n_i$ or n_a are small enough, some terms can be ignored in the sums. Unfortunately, this threshold must be very tight in practice, and this simplification did not provide any noticeable gains for the systems considered in this study. However, this approximation will be absolutely necessary in the limit as $\beta \to \infty$ to prevent overflow.

4. RESULTS

4.1. Benchmark Calculation. In order to validate the implementation of the method and test its accuracy, we report calculations on an exactly solvable system: the Be atom in a minimal basis. It does not make physical sense to consider a vacuum system in the Grand Canonical ensemble, but the model is nonetheless well-defined in a finite basis. This model system involves five spatial orbitals and thus can be solved exactly. In the Grand Canonical ensemble, an exact solution requires, at least in principle, tracing over all possible particle number and spin sectors. In all calculations, we use the orbitals computed at zero temperature.

For this particular system, FT-CCSD performs very well. Figure 2 shows the correlation contribution to the thermody-

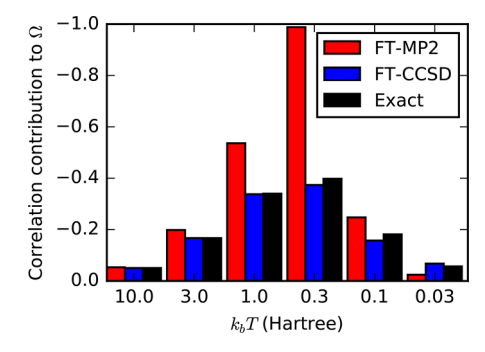


Figure 2. FT-MP2, FT-CCSD, and exact correlation contributions to the grand potential in E_h for the Be model. FT-CCSD, at the worst, underestimates the correlation contribution by ~13%.

namic potential computed with FT-MP2, FT-CCSD, and exact diagonalization. The temperature range was chosen to be high enough that the finite temperature effects are quite significant, but not so high that the noninteracting system becomes exact. FT-CCSD universally outperforms FT-MP2, as we might expect, and the energies are, at worst, in error by 13%. The good

performance of FT-CCSD persists even in the problematic cases where $\Omega^{(2)}$ is a significant overestimate of the exact correlation contribution.

We have also used this model system to study the convergence with respect to the grid used for numerical integration. The relative error in the computed value Ω_{CC} due to numerical integration is shown in Figure 3, as a function of

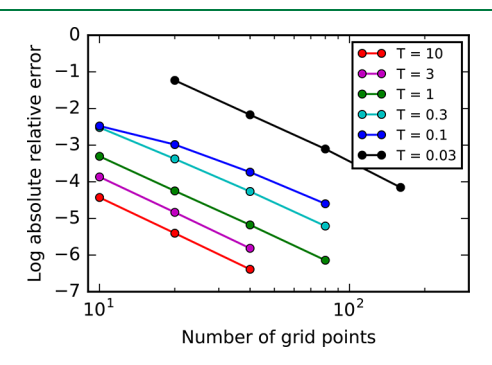


Figure 3. Convergence of the correlation contribution to the grand potential of the Be model, with respect to the size of integration grid for different temperatures.

the number of grid points. The number of grid points required to obtain a specified accuracy is strongly dependent on the temperature. Generally, it will also be dependent on the energy spectrum of the particular problem. In this case, acceptable accuracy can be obtained at high temperatures ($k_{\rm B}T \geq 1.0~E_{\rm h}$) with ~10 grid points. At lower temperatures, more grid points are required, and, in practice, one should ensure convergence of the property of interest, with respect to the quadrature grid. Also, we have observed that the amplitude equations require less damping and converge in fewer iterations when more grid points are used.

4.2. The Uniform Electron Gas at Finite Temperature.

The regime of "warm dense matter" has been the subject of much recent theoretical and experimental interest. 9,37,71 Warm dense matter is loosely characterized by an electron Wigner-Seitz radius (r_e) and reduced temperature $(\theta = k_B T/E_E)$, both of order 1. The theoretical description of matter under these conditions is challenging, because of the similar importance of thermal effects and quantum exchange and correlation. The uniform electron gas at warm dense matter conditions has emerged as an essential test for theory and an ingredient for the parametrization of various flavors of finite temperature DFT. 17,36,72-74 Reference 37 offers a comprehensive review that highlights progress in quantum Monte Carlo (QMC) calculations in particular. In the past, some calculations have been reported in the Grand Canonical ensemble, 72,73,75,76 but recent work has focused on high-quality QMC calculations on both the polarized^{32,77-79} and unpolarized^{32,80,81} UEG in the canonical ensemble. The fixed node approximation of RPIMC is a source of uncontrolled error, 82 and, since the work of Brown et al.,³² there has been considerable effort to obtain more-accurate results over a wider range of r_s . 34,35,77-81,81,83-85 In these studies, the N=33 polarized UEG and N=66unpolarized UEG have emerged as benchmark systems.

In Figure 4, we show the total energy per electron of the unpolarized UEG computed with FT-CCSD for several relevant values of r_s and θ . We use a basis of 57 plane waves, and the chemical potential is adjusted so that N=38. This one-dimensional root finding problem, $N(\mu)-38=0$, is solved with the secant method and takes 4–5 iterations on average. Ten (10) grid points are used for all calculations. The error due to the finite grid will be maximal at low temperatures and at large r_s , but even for $r_s=4$ and $\theta=0.25$, we estimate the impact of this error on the exchange correlation energy be <1%. Comprehensive tables of all our results are given in the Supporting Information, where we also show results for N=14

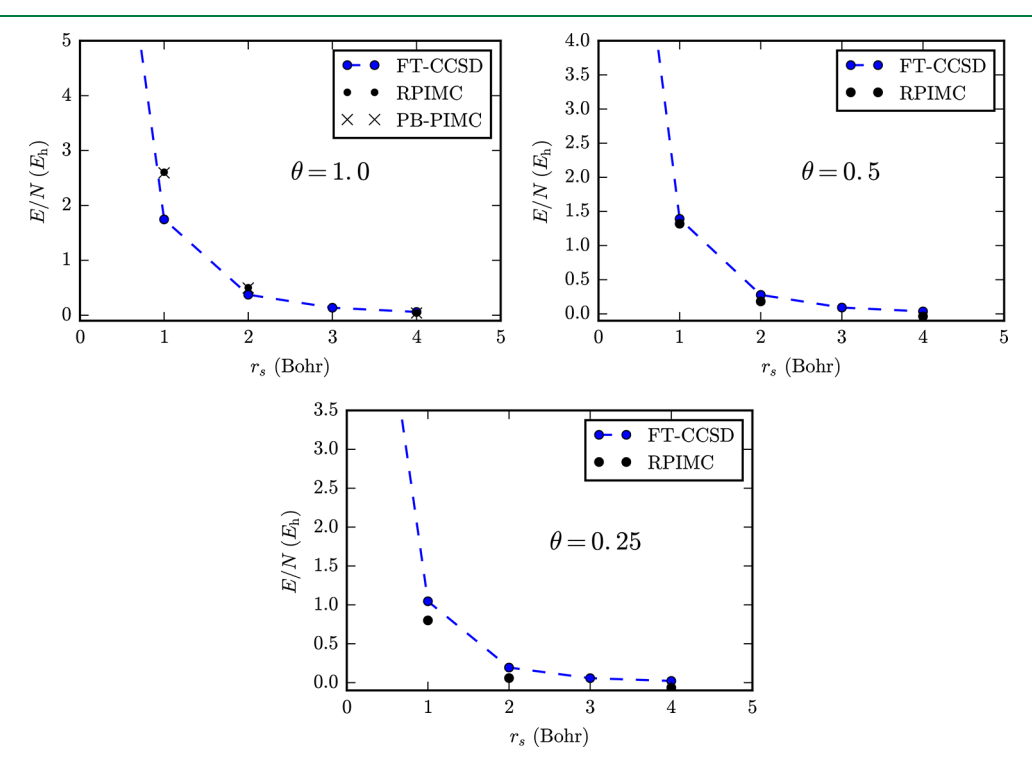


Figure 4. Total energies per electron of the uniform electron gas computed with FT-CCSD. The RPIMC results are those of Brown et al. 32

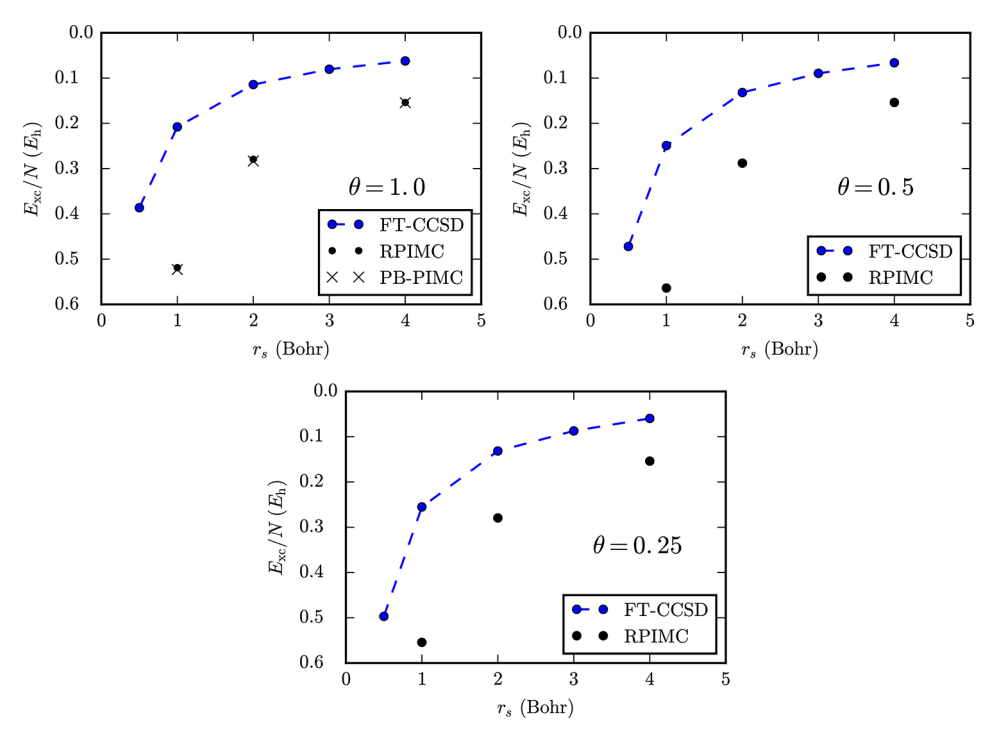


Figure 5. Exchange-correlation energies per electron of the uniform electron gas computed with FT-CCSD. The RPIMC results are those of Brown et al. 32

and N=66 electrons. In Figure 5, we show the exchange-correlation energy for the warm-dense UEG. We also offer comparisons with RPIMC calculations³² for all temperatures and permutation-blocking PIMC⁸¹ for $\theta=1$. Note that, while the fixed node approximation of RPIMC leads to significant errors for the polarized UEG,^{77,84} the fixed node error for the unpolarized UEG is much less severe.⁸¹ Therefore, RPIMC provides a reasonable benchmark for the range of $r_{\rm s}$ values presented here.

Note that the QMC and FT-CCSD calculations compute different quantities, as canonical and Grand Canonical ensemble results will only agree in the thermodynamic limit, and finite -size effects in both cases are large. In addition, the FT-CC works within a (small) orbital basis, while both QMC simulations have no basis-set error. Nonetheless, the comparison between the two shows that the equation of state is qualitatively similar. Thus, as improved implementations of FT-CC appear, we expect it will become a promising tool for the study of warm dense matter.

5. CONCLUSIONS

In this work, we have shown how an explicitly time-dependent formulation of coupled cluster can be used to develop a finite-temperature coupled-cluster theory. The resulting FT-CC theory can be derived directly from many-body perturbation theory and is formally equivalent to the normal-ordered ansatz of the TCC method. In addition to the derivation of the FT-CCSD amplitude equations, we have also shown how first-order properties may be computed as analytic derivatives using a variational Lagrangian. Preliminary calculations on the uniform electron gas show that FT-CC methods are promising candidates for nonperturbative, nonstochastic computation of the properties of quantum systems at finite temperature.

For large-scale application, a variety of practical improvements are still necessary:

- Specialization to restricted reference
- Use of disk to lower memory footprint
- MPI parallelization over time points
- More-stable iteration of the amplitude/ λ equations

These improvements mimic the algorithmic advances that have made efficient, black-box implementation of modern coupled-cluster methods feasible. There is also further room for improvement in the low-temperature regime, where the simple structure of the *S* amplitudes should allow for a reduction of the computational cost.

Finally, note that the time-dependent formulation of coupled cluster presented here is remarkably general. We have shown how it can be used to unify coupled-cluster, thermal-cluster cumulant, and many-body perturbation theories into a computational method well-suited to practical implementation. However, further generalizations including the extension to systems out of equilibrium, are possible and are the subject of current investigation.

■ APPENDIX A: FT-CCSD AMPLITUDE EQUATIONS

The FT-CCSD contribution to the thermodynamic potential, given in eq 8, can be written as

$$\Omega_{\rm CC} = \frac{1}{\beta} \int_0^\beta E(\tau) \tag{A-1}$$

where

$$E(\tau) = \sum_{ia} f_{ia} s_i^a(\tau) + \frac{1}{4} \sum_{ijab} \langle ij||ab \rangle [s_{ij}^{ab}(\tau) + 2s_i^a(\tau) s_j^b(\tau)]$$
(A-2)

Note the analogy to the standard, zero-temperature, coupledcluster energy expression. The singles and doubles equations similarly have the simple form

$$s_i^a(\tau) = -\int_0^{\tau} d\tau' \, e^{(\varepsilon_a - \varepsilon_i)(\tau' - \tau)} S1_i^a(\tau')$$
(A-3)

$$s_{ij}^{ab}(\tau) = -\int_0^{\tau} d\tau' e^{(\epsilon_a + \epsilon_b - \epsilon_i - \epsilon_j)(\tau_{\prime} - \tau)} S2_{ij}^{ab}(\tau')$$
(A-4)

where the integrands *S*1 and *S*2 are precisely the equations of a zero-temperature CCSD iteration, except that each open line that connects to a Hamiltonian fragment carries with it an occupation number:

$$S1_{i}^{a}(\tau') = (1 - n_{a})n_{i}f_{ai} + \sum_{b} (1 - n_{a})f_{ab}s_{i}^{b}(\tau') - \sum_{j} n_{i}f_{ji}s_{j}^{a}(\tau') + \sum_{jb} \langle jallbi\rangle s_{j}^{b}(\tau') + \sum_{jb} f_{jb}s_{ij}^{ab}(\tau')$$

$$+ \frac{1}{2} \sum_{jbc} (1 - n_{a})\langle ajllbc\rangle s_{ij}^{bc}(\tau') - \frac{1}{2} \sum_{jkb} n_{i}\langle jkllib\rangle s_{jk}^{ab}(\tau') - \sum_{jb} f_{jb}s_{i}^{b}(\tau')s_{j}^{a}(\tau') + \sum_{jbc} (1 - n_{a})\langle jallbc\rangle s_{j}^{b}(\tau')s_{i}^{c}(\tau')$$

$$- \sum_{jkb} \langle jkllbi\rangle s_{j}^{b}(\tau')s_{k}^{a}(\tau') - \frac{1}{2} \sum_{jkbc} \langle jkllbc\rangle s_{i}^{b}(\tau')s_{jk}^{ac}(\tau') - \frac{1}{2} \sum_{jkbc} \langle jkllbc\rangle s_{j}^{a}(\tau')s_{ik}^{bc}(\tau') + \sum_{jkbc} \langle jkllbc\rangle s_{j}^{b}(\tau')s_{ki}^{ca}(\tau')$$

$$+ \sum_{jkcd} \langle jkllbc\rangle s_{i}^{b}(\tau')s_{j}^{c}(\tau')s_{k}^{a}(\tau')$$

$$(A-5)$$

$$\begin{split} S2^{ab}_{ij}(\tau') &= n_{i}n_{j}(1-n_{a})(1-n_{b})\langle abllij\rangle + P(ij) \sum_{c} n_{j}(1-n_{a})(1-n_{b})\langle abllicj\rangle s_{i}^{c}(\tau') - P(ab) \sum_{k} n_{i}n_{j}(1-n_{b})\langle kbllij\rangle s_{k}^{a}(\tau') \\ &+ P(ab) \sum_{c} (1-n_{b})f_{bc} s_{ij}^{ac}(\tau') - P(ij) \sum_{k} n_{j}f_{kj} s_{ik}^{ab}(\tau') + \frac{1}{2} \sum_{cd} (1-n_{a})(1-n_{b})\langle abllcd\rangle s_{ij}^{cd}(\tau') + \frac{1}{2} \sum_{kl} n_{i}n_{j}\langle klllij\rangle s_{k}^{ab}(\tau') \\ &+ P(ij)P(ab) \sum_{kc} n_{j}(1-n_{b})\langle kbllcj\rangle s_{ik}^{ac}(\tau') + \frac{1}{2}P(ij) \sum_{cd} (1-n_{a})(1-n_{b})\langle abllcd\rangle s_{i}^{c}(\tau') s_{i}^{d}(\tau') + \frac{1}{2}P(ab) \sum_{kl} n_{i}n_{j}\langle klllij\rangle s_{k}^{a}(\tau') s_{i}^{b}(\tau') \\ &- P(ij)P(ab) \sum_{kc} (1-n_{a})n_{j}\langle akllcj\rangle s_{i}^{c}(\tau') s_{k}^{b}(\tau') - P(ij) \sum_{kc} f_{kc} s_{i}^{c}(\tau') s_{ij}^{ab}(\tau') - P(ab) \sum_{kc} f_{kc} s_{i}^{c}(\tau') s_{ij}^{ab}(\tau') \\ &+ P(ab) \sum_{kcd} (1-n_{a})\langle kallcd\rangle s_{i}^{c}(\tau') s_{ij}^{ab}(\tau') - P(ij) \sum_{kl} n_{i}\langle klllci\rangle s_{i}^{c}(\tau') s_{ij}^{ab}(\tau') + P(ij)P(ab) \sum_{kcd} (1-n_{a})\langle akllcd\rangle s_{i}^{c}(\tau') s_{ij}^{ab}(\tau') \\ &- P(ij)P(ab) \sum_{klc} n_{i}\langle klllicl\rangle s_{i}^{a}(\tau') s_{ij}^{ab}(\tau') + \frac{1}{2}P(ij) \sum_{klc} n_{i}\langle klllci\rangle s_{i}^{c}(\tau') s_{ij}^{ab}(\tau') - \frac{1}{2}P(ab) \sum_{kcd} (1-n_{a})\langle akllcd\rangle s_{i}^{c}(\tau') s_{ij}^{ab}(\tau') \\ &+ \frac{1}{4} \sum_{klcd} \langle klllcd\rangle s_{i}^{c}(\tau') s_{ij}^{ab}(\tau') + \frac{1}{2}P(ij)P(ab) \sum_{klcd} \langle klllcd\rangle s_{i}^{c}(\tau') s_{ij}^{ab}(\tau') - \frac{1}{2}P(ab) \sum_{klcd} \langle klllcd\rangle s_{kl}^{c}(\tau') s_{ij}^{ab}(\tau') \\ &+ \frac{1}{2}P(ij)\sum_{klcd} \langle klllcd\rangle s_{i}^{c}(\tau') s_{i}^{a}(\tau') s_{i}^{b}(\tau') - \frac{1}{2}P(ij)P(ab) \sum_{klcd} \langle klllcd\rangle s_{i}^{c}(\tau') s_{i}^{a}(\tau') s_{ij}^{a}(\tau') \\ &+ \frac{1}{4}P(ab) \sum_{klcd} \langle klllcd\rangle s_{i}^{c}(\tau') s_{i}^{a}(\tau') s_{i}^{b}(\tau') - P(ab) \sum_{klcd} \langle klllcd\rangle s_{i}^{c}(\tau') s_{i}^{a}(\tau') s_{ij}^{a}(\tau') \\ &+ \frac{1}{4}P(ab) \sum_{klcd} \langle klllcd\rangle s_{i}^{c}(\tau') s_{i}^{a}(\tau') s_{i}^{b}(\tau') - P(ab) \sum_{klcd} \langle klllcd\rangle s_{i}^{c}(\tau') s_{i}^{a}(\tau') s_{ij}^{a}(\tau') \\ &+ \frac{1}{4}P(ab) \sum_{klcd} \langle klllcd\rangle s_{i}^{c}(\tau') s_{i}^{a}(\tau') s_{i}^{b}(\tau') - P(ab) \sum_{klcd} \langle klllcd\rangle s_{i}^{c}(\tau') s_{i}^{a}(\tau') s_{ij}^{a}(\tau') \\ &+ \frac{1}{4}P(ij)P(ab) \sum_{klcd} \langle klllcd\rangle s_{i}^{c}(\tau') s_{i$$

These expressions are most easily obtained using the rules given in Section 2.1. Note that the Fock matrix, f, is meant to represent only the first-order part and therefore does not include the diagonal (orbital energies).

APPENDIX B: RULES FOR FINITE-TEMPERATURE, DIAGRAMMATIC PERTURBATION THEORY

The contributions to the free energy at some finite order, *n*, in perturbation theory can be enumerated in the time domain by a diagrammatic procedure. There are many different methods for this purpose, but we will use diagrams that mimic the antisymmetrized Goldstone diagrams common in quantum chemistry. We will imagine a time axis going from bottom to top and the basic diagrammatic components are the same as

those described in Chapter 4 of ref 53. The *n*th-order contribution to the shift in the grand potential can be obtained by the following procedure:

- (1) Draw all topologically distinct diagrams with n interactions. Diagrams differing by the time order of non-equivalent interactions are considered distinct, as with other types of Goldstone diagrams.
 - (2) Associate a unique orbital index with each directed line.
- (3) Associate a unique imaginary time $(\tau_1, \tau_2, ...)$ with each interaction.
- (4) With each one-electron interaction, associate a factor such as $f_{pq} \mathrm{e}^{(\varepsilon_p \varepsilon_q) \tau}$, where p is the index of the outgoing line, q is the index of the incoming line, and τ is the time associated with the particular interaction.

- (5) With each two-electron interaction, associate a factor such as $\langle pq|lrs \rangle f_{pq} \mathrm{e}^{(\varepsilon_p + \varepsilon_q \varepsilon_r \varepsilon_s)\tau}$, where p,q,r, and s are the indices of the left outgoing, right outgoing, left incoming, and right incoming lines, respectively. τ is the time associated with the interaction.
- (6) Integrate each intermediate time from 0 to the next labeled time. The final time is integrated from 0 to β :

$$\int_0^\beta d\tau_f ... \int_0^{\tau_3} d\tau_2 \int_0^{\tau_2} d\tau_1 ...$$
 (B-1)

- (7) Sum over all orbital indices.
- (8) Multiply the overall diagram by a factor of $(-1)^{n-1}(-1)^{l+h}/\beta$, where l is the number of closed loops and h is the number of hole lines.
- (9) For antisymmetrized diagrams divide by 2^s, where s is the number of pairs of equivalent Fermion lines. If the standard (direct) interactions are used, the diagram should be divided by 2 if it is symmetric, with respect to reflection across a vertical line.

These rules can be used, at least in theory, to derive explicit expressions for the shift in the grand potential at any finite order in perturbation theory. In practice, performing the time integrals becomes increasingly cumbersome at higher order. This method can be viewed as an alternative to the frequency space method, which will involve the evaluation of Matsubara sums.

\blacksquare APPENDIX C: THE FT-CCSD λ EQUATIONS

The implementation of the FT-CCSD λ -equations mirrors that of the zero-temperature theory, but we must explicitly take into account the numerical integration scheme in order to faithfully reproduce finite-difference differentiation (see Appendix D for the notation and details pertaining to the numerical integration). Using a vector notation, the Lagrangian can be written as

$$\mathcal{L} = \frac{1}{\beta} g_{y} E^{y} [\mathbf{s}^{y}] - \frac{1}{\beta} g_{y} \lambda^{y} \cdot \{ \mathbf{s}^{y} + G_{x}^{y} e^{\Delta(\tau^{x} - \tau^{y})} \mathbf{S}^{x} [\mathbf{s}^{x}] \}$$
 (C-1)

where we have used the fact that all terms in the amplitude equations are evaluated at the same time. Taking the derivative, with respect to a particular amplitude at a specific time point (s_{μ}^{x}) , yields an equation for the λ -amplitudes:

$$\lambda^{\mu x} = \frac{\partial E[\mathbf{s}^x]}{\partial s_{\mu}^x} - g_y \lambda^{\nu y} \left(\frac{G_x^y}{g_x}\right) e^{\Delta_{\nu}(\tau^x - \tau^y)} \frac{\partial S_{\nu}^x[\mathbf{s}^x]}{\partial s_{\mu}^x}$$
(C-2)

where we have used index notation with implied summations. If we define a quantity

$$\widetilde{\lambda}_{x}^{\nu} \equiv g_{y} \lambda^{\nu y} \left(\frac{G_{x}^{y}}{g_{x}} \right) e^{\Delta_{\nu} (\tau^{x} - \tau^{y})} \tag{C-3}$$

we can write the λ equations in a form closely resembling the zero-temperature analogue:

$$\lambda^{\mu x} = \frac{\partial E[\mathbf{s}^x]}{\partial s^x_{\mu}} - \tilde{\lambda}^{\nu}_{x} \frac{\partial S^x_{\nu}[\mathbf{s}^x]}{\partial s^x_{\mu}}$$
(C-4)

Since the amplitude equations are diagrammatically identical to the zero-temperature amplitude equations, the λ equations will also involve the same diagrams. The only difference is that we must in each iteration first compute $\tilde{\lambda}$ from λ and then compute the new λ amplitudes at each time point. Properties

can then be evaluated by evaluating \mathcal{L} with the appropriate derivative integrals. For E, S, and N, we require derivatives of the occupation numbers with respect to μ and β :

$$\frac{\partial n_p}{\partial \mu} = \beta n_p (1 - n_p) \qquad \frac{\partial n_p}{\partial \beta} = (\mu - \varepsilon_p) n_p (1 - n_p)$$
(C-5)

As in the zero-temperature formulation, this final step can be accomplished by contraction with response-density tensors.

A slight complication arises when derivatives, with respect to β (or T), are required. In this case, we must also consider the terms which are proportional to the derivatives of g and G, which will generally be dependent on β . The specific form of these derivatives will be dependent on the particular quadrature scheme. In this study, we have used Simpson's rule on a uniform grid, which makes these terms simple to compute. Finally, there will some contributions from the locations of the grid points, which will be dependent on β . These contributions will vanish in the limit of a dense grid, but are necessary to faithfully reproduce the finite difference derivatives when using a small number of grid points.

APPENDIX D: NUMERICAL INTEGRATION

Our implementation is general enough to use a generic numerical quadrature. A function, $I(\tau)$, evaluated at the grid points, will be indicated as $I_x \equiv I(\tau_x)$; the n roots are labeled by x, y, \dots Integrals are then approximated as

$$\int_0^\beta I(\tau) \, d\tau \approx \sum_x g^x I_x \tag{D-1}$$

$$\int_0^{\tau_y} I(\tau) d\tau \approx \sum_x G_y^x I_x \tag{D-2}$$

where g and G are the tensors of weights.

In this study, we have employed a uniform grid for the sake of simplicity. For n grid points, the first grid point is located at $\tau = 0$, the last is located at $\tau = \beta$, and the spacing between the points is given by $\delta = \beta/(n-1)$. Simpson's rule is used for all integrations:

$$\int_0^a I(\tau) d\tau = \frac{\delta}{3} [I_1 + 4I_2 + 2I_3 + 4I_4 + \dots + I_n]$$
 (D-3)

This defines the weights \mathbf{g} and \mathbf{G} . The uniform grid means that we only need to perform integrals from 0 to a, where a is a grid point, and no interpolation is required.

To compute thermodynamic quantities, we furthermore require the derivatives of the weight tensors, with respect to β . Since the elements of these tensors are all linear in β , the derivative is trivial.

ASSOCIATED CONTENT

S Supporting Information

The Supporting Information is available free of charge on the ACS Publications website at DOI: 10.1021/acs.jctc.8b00773.

Raw data on the warm dense UEG (PDF)

AUTHOR INFORMATION

Corresponding Authors

*E-mail: whiteaf@berkeley.edu (A. F. White).

*E-mail: gkc1000@gmail.com (G. K.-L. Chan).

ORCID ®

Alec F. White: 0000-0002-9743-1469

The authors declare no competing financial interest.

ACKNOWLEDGMENTS

The authors would like to thank Jiajun Ren for helpful discussions. This work is supported by the U.S. Department of Energy, Office of Science, via Grant No. SC0018140.

REFERENCES

- (1) Jarrell, M.; Maier, T.; Hettler, M. H.; Tahvildarzadeh, A. N. Phase diagram of the Hubbard model: Beyond the dynamical mean field. EPL 2001, 56, 563-569.
- (2) Macridin, A.; Jarrell, M.; Maier, T.; Sawatzky, G. A. Physics of cuprates with the two-band Hubbard model: The validity of the oneband Hubbard model. Phys. Rev. B: Condens. Matter Mater. Phys. 2005,
- (3) Maier, T. A.; Jarrell, M.; Schulthess, T. C.; Kent, P. R. C.; White, J. B. Systematic study of d-wave superconductivity in the 2D repulsive Hubbard model. Phys. Rev. Lett. 2005, 95, 237001.
- (4) Yang, S. X.; Fotso, H.; Su, S. Q.; Galanakis, D.; Khatami, E.; She, J. H.; Moreno, J.; Zaanen, J.; Jarrell, M. Proximity of the superconducting dome and the quantum critical point in the twodimensional Hubbard model. Phys. Rev. Lett. 2011, 106, 047004.
- (5) Gull, E.; Parcollet, O.; Millis, A. J. Superconductivity and the pseudogap in the two-dimensional hubbard model. Phys. Rev. Lett. 2013, 110, 216405.
- (6) Bousseksou, A.; Molnár, G.; Salmon, L.; Nicolazzi, W. Molecular spin crossover phenomenon: recent achievements and prospects. Chem. Soc. Rev. 2011, 40, 3313-3335.
- (7) Moroni, E. G.; Grimvall, G.; Jarlborg, T. Free energy contributions to the hcp-bcc transformation in transition metals. Phys. Rev. Lett. 1996, 76, 2758-2761.
- (8) Mukherjee, S.; Libisch, F.; Large, N.; Neumann, O.; Brown, L. V.; Cheng, J.; Lassiter, J. B.; Carter, E. A.; Nordlander, P.; Halas, N. J. Hot electrons do the impossible: Plasmon-induced dissociation of H₂ on Au. Nano Lett. 2013, 13, 240-247.
- (9) Fortov, V. E. Extreme states of matter on Earth and in space. Phys.-Usp. 2009, 52, 615-647.
- (10) Ernstorfer, R.; Harb, M.; Hebeisen, C. T.; Sciaini, G.; Dartigalongue, T.; Miller, R. J. D. The formation of warm dense matter: Experimental evidence for electronic bond hardening in gold. Science 2009, 323, 1033-1037.
- (11) Mermin, N. D. Stability of the thermal Hartree-Fock approximation. Ann. Phys. 1963, 21, 99-121.
- (12) Mermin, N. D. Thermal properties of the inhomogeneous electron gas. Phys. Rev. 1965, 137, A1441-A1443.
- (13) Stoitsov, M.; Petkov, I. Density functional theory at finite temperatures. Ann. Phys. 1988, 184, 121-147.
- (14) Eschrig, H. T > 0 ensemble-state density functional theory via Legendre transform. Phys. Rev. B: Condens. Matter Mater. Phys. 2010,
- (15) Pittalis, S.; Proetto, C. R.; Floris, A.; Sanna, A.; Bersier, C.; Burke, K.; Gross, E. K. U. Exact conditions in finite-temperature density-functional theory. Phys. Rev. Lett. 2011, 107, 163001.
- (16) Cytter, Y.; Rabani, E.; Neuhauser, D.; Baer, R. Stochastic density functional theory at finite temperatures. Phys. Rev. B: Condens. Matter Mater. Phys. 2018, 97, 115207.
- (17) Karasiev, V. V.; Dufty, J. W.; Trickey, S. B. Nonempirical Semilocal Free-Energy Density Functional for Matter under Extreme Conditions. Phys. Rev. Lett. 2018, 120, 76401.
- (18) Fetter, A. L.; Walecka, J. D. Quantum Theory of Many-Particle Systems; Dover Publications: Mineola, NY, 2003.
- (19) Blaizot, J.-P.; Ripka, G. Quantum Theory of Finite Systems; The MIT Press: Cambridge, MA, 1985.

- (20) Negele, J. W.; Orland, H. Quantum Many-Particle Systems; Addison-Wesley: Redwood City, CA, 1987.
- (21) Kananenka, A. A.; Welden, A. R.; Lan, T. N.; Gull, E.; Zgid, D. Efficient temperature-dependent Green's function methods for realistic systems: Using cubic spline interpolation to approximate Matsubara Green's functions. J. Chem. Theory Comput. 2016, 12, 2250-2259.
- (22) Welden, A. R.; Rusakov, A. A.; Zgid, D. Exploring connections between statistical mechanics and Green's functions for realistic systems: Temperature dependent electronic entropy and internal energy from a self-consistent second-order Green's function. J. Chem. Phys. 2016, 145, 204106.
- (23) Georges, A.; Kotliar, G.; Krauth, W.; Rozenberg, M. J. Dynamical mean-field theory of strongly correlated fermion systems and the limit of infinite dimensions. Rev. Mod. Phys. 1996, 68, 13.
- (24) Kotliar, G.; Savrasov, S. Y.; Haule, K.; Oudovenko, V. S.; Parcollet, O.; Marianetti, C. A. Electronic structure calculations with dynamical mean-field theory. Rev. Mod. Phys. 2006, 78, 865-951.
- (25) Hettler, M.; Tahvildar-Zadeh, A.; Jarrell, M.; Pruschke, T.; Krishnamurthy, H. R. Nonlocal dynamical correlations of strongly interacting electron systems. Phys. Rev. B: Condens. Matter Mater. Phys. 1998, 58, R7475-R7479.
- (26) Blankenbecler, R.; Scalapino, D.; Sugar, R. Monte Carlo calculations of coupled boson-fermion systems. Phys. Rev. D: Part. Fields 1981, 24, 2278.
- (27) Liu, Y.; Cho, M.; Rubenstein, B. Ab Initio Finite Temperature Auxiliary Field Quantum Monte Carlo. J. Chem. Theory Comput. 2018, 14, 4722-4732.
- (28) Chandler, D.; Wolynes, P. G. Exploiting the isomorphism between quantum theory and classical statistical mechanics of polyatomic fluids. J. Chem. Phys. 1981, 74, 4078-4095.
- (29) Ceperley, D. M. Path integrals in the theory of condensed helium. Rev. Mod. Phys. 1995, 67, 279-355.
- (30) Militzer, B.; Ceperley, D. M. Path integral monte carlo calculation of the deuterium hugoniot. Phys. Rev. Lett. 2000, 85, 1890-1893.
- (31) Ceperley, D. M. Fermion nodes. J. Stat. Phys. 1991, 63, 1237-1267
- (32) Brown, E. W.; Clark, B. K.; Dubois, J. L.; Ceperley, D. M. Pathintegral Monte Carlo simulation of the warm dense homogeneous electron gas. Phys. Rev. Lett. 2013, 110, 146405.
- (33) Schoof, T.; Bonitz, M.; Filinov, A.; Hochstuhl, D.; Dufty, J. W. Configuration path integral Monte Carlo. Contrib. Plasma Phys. 2011, 51, 687-697.
- (34) Blunt, N. S.; Rogers, T. W.; Spencer, J. S.; Foulkes, W. M. C. Density-matrix quantum Monte Carlo method. Phys. Rev. B: Condens. Matter Mater. Phys. 2014, 89, 245124.
- (35) Malone, F. D.; Blunt, N. S.; Shepherd, J. J.; Lee, D. K.; Spencer, J. S.; Foulkes, W. M. Interaction picture density matrix quantum Monte Carlo, I. Chem. Phys. 2015, 143, 044116.
- (36) Karasiev, V. V.; Sjostrom, T.; Dufty, J.; Trickey, S. B. Accurate homogeneous electron gas exchange-correlation free energy for local spin-density calculations. Phys. Rev. Lett. 2014, 112, 076403.
- (37) Dornheim, T.; Groth, S.; Bonitz, M. The uniform electron gas at warm dense matter conditions. Phys. Rep. 2018, 744, 1-86.
- (38) Paldus, J.; Cízek, J.; Shavitt, I. Correlation problems in atomic and molecular systems. IV. Extended coupled-pair many-electron theory and its application to the BH3 molecule. Phys. Rev. A: At., Mol., Opt. Phys. 1972, 5, 50-67.
- (39) Bartlett, R. J. Many-body perturbation theory and coupled cluster theory for electron correlation in molecules. Annu. Rev. Phys. Chem. 1981, 32, 359-401.
- (40) Farnell, D. J. J.; Bishop, R. F. In Quantum Magnetism; Schollwöck, U., Richter, J., Farnell, D. J., Bishop, R. F., Eds.; Springer: Berlin, Heidelberg, Germany, 2004; pp 307-348.
- (41) Bartlett, R. J.; Musiał, M. Coupled-cluster theory in quantum chemistry. Rev. Mod. Phys. 2007, 79, 291-352.

- (42) Booth, G. H.; Grüneis, A.; Kresse, G.; Alavi, A. Towards an exact description of electronic wavefunctions in real solids. *Nature* **2012**, 493, 365–370.
- (43) Kaulfuss, U. B.; Altenbokum, M. Anharmonic oscillator as a test of the coupled cluster method. *Phys. Rev. D: Part. Fields* **1986**, 33, 3658–3664.
- (44) Sanyal, G.; Mandal, S. H.; Mukherjee, D. Thermal averaging in quantum many-body systems: a non-perturbative thermal cluster cumulant approach. *Chem. Phys. Lett.* **1992**, *192*, 55–61.
- (45) Sanyal, G.; Mandal, S. H.; Guha, S.; Mukherjee, D. Systematic nonperturbative approach for thermal averages in quantum many-body systems: The thermal-cluster-cumulant method. *Phys. Rev. E: Stat. Phys., Plasmas, Fluids, Relat. Interdiscip. Top.* **1993**, *48*, 3373–3389.
- (46) Mandal, S. H.; Ghosh, R.; Mukherjee, D. A non-perturbative cumulant expansion method for the grand partition function of quantum systems. *Chem. Phys. Lett.* **2001**, 335, 281–288.
- (47) Mandal, S. H.; Ghosh, R.; Sanyal, G.; Mukherjee, D. A non-perturbative path-integral based thermal cluster expansion approach for grand partition function of quantum systems. *Chem. Phys. Lett.* **2002**, 352, 63–69.
- (48) Mandal, S. H.; Ghosh, R.; Sanyal, G.; Mukherjee, D. A finite-temperature generalisation of the coupled cluster method: A Non-perturbative access to grand partition functions. *Int. J. Mod. Phys. B* **2003**, *17*, 5367–5377.
- (49) Hermes, M. R.; Hirata, S. Finite-temperature coupled-cluster, many-body perturbation, and restricted and unrestricted Hartree-Fock study on one-dimensional solids: Luttinger liquids, Peierls transitions, and spin- and charge-density waves. *J. Chem. Phys.* **2015**, *143*, 102818.
- (50) Hirata, S.; He, X. On the Kohn-Luttinger conundrum. *J. Chem. Phys.* **2013**, *138*, 204112.
- (51) Hummel, F. Finite temperature coupled cluster theories for extended systems. arXiv:1807.09687, 2018.
- (52) Helgaker, T.; Jørgensen, P.; Olsen, J. *Molecular Electronic Structure Theory*; John Wiley and Sons, Inc.: Chichester, West Sussex, England, 2000.
- (53) Shavitt, I.; Bartlett, R. J. Many-Body Methods in Chemistry and Physics: MBPT and Coupled-Cluster Theory; Cambridge University Press: New York, 2009.
- (54) Janssen, C. L.; Schaefer, H. F. The automated solution of second quantization equations with applications to the coupled cluster approach. *Theor. Chim. Acta.* **1991**, *79*, 1–42.
- (55) Hirata, S. Tensor contraction engine: Abstraction and automated parallel implementation of configuration-interaction, coupled-cluster, and many-body perturbation theories. *J. Phys. Chem.* A 2003, 107, 9887–9897.
- (56) Schönhammer, K.; Gunnarsson, O. Time-dependent approach to the calculation of spectral functions. *Phys. Rev. B: Condens. Matter Mater. Phys.* **1978**, 18, 6606–6614.
- (57) Hoodbhoy, P.; Negele, J. W. Time-dependent coupled-cluster approximation to nuclear dynamics. I. Application to a solvable model. *Phys. Rev. C: Nucl. Phys.* **1978**, *18*, 2380–2394.
- (58) Huber, C.; Klamroth, T. Explicitly time-dependent coupled cluster singles doubles calculations of laser-driven many-electron dynamics. *J. Chem. Phys.* **2011**, *134*, 054113.
- (59) Kvaal, S. Ab initio quantum dynamics using coupled-cluster. J. Chem. Phys. 2012, 136, 194109.
- (60) Nascimento, D. R.; DePrince, A. E. Linear absorption spectra from explicitly time-dependent equation-of-motion coupled-cluster theory. *J. Chem. Theory Comput.* **2016**, *12*, 5834–5840.
- (61) Szabo, A.; Ostlund, N. Modern Quantum Chemistry; McGraw-Hill: New York, 1982; p 107.
- (62) Gross, E. K. U.; Runge, E. Many-Particle Theory; IOP Publishing: New York, 1991.
- (63) Kohn, W.; Luttinger, J. M. Ground-state energy of a Many-Fermion system. *Phys. Rev.* **1960**, *118*, 41–45.
- (64) Santra, R.; Schirmer, J. Finite-temperature second-order many-body perturbation theory revisited. *Chem. Phys.* **2017**, 482, 355.

- (65) Salter, E. A.; Trucks, G. W.; Bartlett, R. J. Analytic energy derivatives in many-body methods. I. First derivatives. *J. Chem. Phys.* **1989**, *90*, 1752–1766.
- (66) Sun, Q.; Berkelbach, T. C.; Blunt, N. S.; Booth, G. H.; Guo, S.; Li, Z.; Liu, J.; McClain, J. D.; Sayfutyarova, E. R.; Sharma, S.; Wouters, S.; Chan, G. K. L. PySCF: the Python-based simulations of chemistry framework. *Wiley Interdiscip. Rev. Comput. Mol. Sci.* **2018**, 8, e1340.
- (67) Pulay, P. Convergence acceleration of iterative sequences. The case of SCF iteration. *Chem. Phys. Lett.* **1980**, *73*, 393–398.
- (68) Pulay, P. Improved SCF convergence acceleration. J. Comput. Chem. 1982, 3, 556–560.
- (69) Scuseria, G. E.; Lee, T. J.; Schaefer, H. F. Accelerating the convergence of the coupled-cluster approach. The use of the DIIS method. *Chem. Phys. Lett.* **1986**, *130*, 236–239.
- (70) Stanton, J. F.; Gauss, J.; Watts, J. D.; Bartlett, R. J. A direct product decomposition approach for symmetry exploitation in many-body methods. I. Energy calculations. *J. Chem. Phys.* **1991**, *94*, 4334–4345.
- (71) Shukla, P. K.; Eliasson, B. Colloquium: Nonlinear collective interactions in quantum plasmas with degenerate electron fluids. *Rev. Mod. Phys.* **2011**, 83, 885–906.
- (72) Gupta, U.; Rajagopal, A. K. Exchange-correlation potential for inhomogeneous electron systems at finite temperatures. *Phys. Rev. A: At., Mol., Opt. Phys.* **1980**, 22, 2792–2797.
- (73) Dharma-Wardana, M. W.; Taylor, R. Exchange and correlation potentials for finite temperature quantum calculations at intermediate degeneracies. *J. Phys. C: Solid State Phys.* **1981**, *14*, 629–646.
- (74) Karasiev, V. V.; Calderín, L.; Trickey, S. B. Importance of finite-temperature exchange correlation for warm dense matter calculations. *Phys. Rev. E: Stat. Phys., Plasmas, Fluids, Relat. Interdiscip. Top.* **2016**, 93, 063207.
- (75) Perrot, F.; Dharma-Wardana, M. W. C. Exchange and correlation potentials for electron-ion systems at finite temperatures. *Phys. Rev. A: At., Mol., Opt. Phys.* **1984**, *30*, 2619–2626.
- (76) Schweng, H. K.; Bohm, H. M.; Schinner, A.; Macke, W. Temperature dependence of short-range correlations in the homogeneous electron gas. *Phys. Rev. B: Condens. Matter Mater. Phys.* **1991**, 44, 13291–13297.
- (77) Schoof, T.; Groth, S.; Vorberger, J.; Bonitz, M. Ab Initio Thermodynamic Results for the Degenerate Electron Gas at Finite Temperature. *Phys. Rev. Lett.* **2015**, *115*, 130402.
- (78) Groth, S.; Schoof, T.; Dornheim, T.; Bonitz, M. Ab initio quantum Monte Carlo simulations of the uniform electron gas without fixed nodes. *Phys. Rev. B: Condens. Matter Mater. Phys.* **2016**, 93, 085102.
- (79) Malone, F. D.; Blunt, N. S.; Brown, E. W.; Lee, D. K.; Spencer, J. S.; Foulkes, W. M.; Shepherd, J. J. Accurate exchange-correlation energies for the warm dense electron gas. *Phys. Rev. Lett.* **2016**, *117*, 115701.
- (80) Dornheim, T.; Groth, S.; Sjostrom, T.; Malone, F. D.; Foulkes, W. M.; Bonitz, M. Ab initio quantum Monte Carlo simulation of the warm dense electron gas in the thermodynamic limit. *Phys. Rev. Lett.* **2016**, *117*, 156403.
- (81) Dornheim, T.; Groth, S.; Schoof, T.; Hann, C.; Bonitz, M. Ab initio quantum Monte Carlo simulations of the uniform electron gas without fixed nodes: The unpolarized case. *Phys. Rev. B: Condens. Matter Mater. Phys.* **2016**, 93, 205134.
- (82) Filinov, V. S. Analytical contradictions of the fixed-node density matrix. *High Temp.* **2014**, *52*, *615*–*620*.
- (83) Filinov, V. S.; Fortov, V. E.; Bonitz, M.; Moldabekov, Z. Fermionic path-integral Monte Carlo results for the uniform electron gas at finite temperature. *Phys. Rev. E* **2015**, *91*, 033108.
- (84) Dornheim, T.; Schoof, T.; Groth, S.; Filinov, A.; Bonitz, M. Permutation blocking path integral Monte Carlo approach to the uniform electron gas at finite temperature. *J. Chem. Phys.* **2015**, *143*, 204101.
- (85) Schoof, T.; Groth, S.; Bonitz, M. Towards ab initio thermodynamics of the electron gas at strong degeneracy. *Contrib. Plasma Phys.* **2015**, *55*, 136–143.